



1     **Microbial Community Structure and Activity Changes in Response**  
2                     **to the Development of Hypoxia in a Shallow Estuary**

3

4

5                     Yunjung Park<sup>1</sup>, Sujin Kim<sup>1</sup>, Soonja Cho<sup>1</sup>, Jaeho Cha<sup>1,2\*</sup> and Soonmo An<sup>3\*</sup>

6

7                     <sup>1</sup>Department of Microbiology, College of Natural Sciences, Pusan National University, Busan

8                     46241, Republic of Korea, <sup>2</sup>Microbiological Resource Research Institute, Pusan National

9                     University, Busan 46241, Republic of Korea, <sup>3</sup>Department of Oceanography, College of Natural

10                     Sciences, Pusan National University, Busan 46241, Republic of Korea

11

12     **Correspondence:**

13     Jaeho Cha, ([jhcha@pusan.ac.kr](mailto:jhcha@pusan.ac.kr))

14     Soonmo An, ([sman@pusan.ac.kr](mailto:sman@pusan.ac.kr))



15 **Abstract.**

16 We examined the effects of changing from oxic to anoxic conditions on microbial communities  
17 using both biogeochemical and molecular approaches in a semi-enclosed estuary (Jinhae Bay,  
18 Republic of Korea). Total microbial activity, represented by oxygen demand in the water column  
19 (WOD) or sediment (SOD), revealed that the respective microbial communities in the water and  
20 sediment responded differently to low dissolved-oxygen (DO) conditions. In the sediment, SOD  
21 and the total microbial abundance, as assessed by quantitative polymerase chain reaction (qPCR)  
22 analysis, decreased under low DO conditions, indicating that the microbial adaptation to  
23 anaerobic metabolism was not well established during hypoxia development. In the water  
24 column, however, neither the total abundance of microbes nor the WOD were affected by  
25 hypoxic conditions. Regardless of DO concentration, WOD showed a positive correlation with  
26 water temperature, implying that the aerobic metabolism was sustained even under hypoxic  
27 conditions, through the intermittent supply of oxygen. In addition to the spatially different  
28 responses of microorganisms, unique responses of specific groups were noted in sulfur (S) and  
29 nitrogen (N) cycling microbes. Sulfide-oxidizing prokaryotes (SOP) dominated in the water  
30 column, and no significant changes were evident in their abundance or diversity with hypoxia.  
31 However, in sediment, distinctive sulfate-reducing bacteria (SRB) were present at each sampling  
32 period during hypoxia development (a “SRB succession”), implying that each SRB group has  
33 varying sensitivity to DO and other electron acceptors. Our results illustrated similarities in  
34 composition and activity of N-cycling microbes between the seasonal hypoxia and permanent  
35 oxygen minimum zone (OMZ). Vertical profiles of dissolved inorganic nitrogen, including  
36 ammonium ( $\text{NH}_4^+$ ) and nitrate ( $\text{NO}_3^-$ ), and changes in archaeal abundance indicated that the  
37  $\text{NH}_4^+$ -oxidizing archaea (AOA) varied spatially and temporally, depending on  $\text{NH}_4^+$  and oxygen



38 availability in the water column, under mature hypoxic conditions. The intriguing N dynamics  
39 recently discovered in the OMZ might also be important in the coastal hypoxic zone.

40

#### 41 **1 Introduction**

42 Human influences on the coastal environment are increasing as a result of industrial and urban  
43 development and pollution (Nogales et al., 2011). Cultural eutrophication and the consequences  
44 of anthropogenic influences cause undesirable algal bloom and hypoxic water (Diaz and  
45 Rosenberg, 2009; Lee et al., 2017). The development of seasonal hypoxia has increased globally,  
46 and has negative economic and environmental consequences (Diaz and Rosenberg, 2008; Naqvi  
47 et al., 2010).

48 Microbes function in the biogeochemical cycling of essential elements, including carbon,  
49 nitrogen, phosphate, and sulfur; hence, the response of microbial communities to low-dissolved-  
50 oxygen (DO) conditions has implications for both coastal management and the global  
51 environment (Ward et al., 2011; Abell et al., 2011). However, detailed microbial ecology studies  
52 on microbial responses to oxygen depletion have been conducted mostly on permanent-oxygen-  
53 minimum zones (OMZ) of open ocean areas, such as the Eastern Tropical North Pacific (ETNP),  
54 Eastern South Pacific (ESP), Northern Indian Ocean, and Arabian Sea (Ulloa et al., 2012; Jensen  
55 et al., 2011). Interactions between microbial nitrogen-removal processes (anaerobic ammonium  
56  $(\text{NH}_4^+)$  oxidation [anammox] and denitrification) and other nitrogen-related processes (e.g.  
57 dissimilatory nitrate  $(\text{NO}_3^-)$  reduction to  $\text{NH}_4^+$  [DNRA] and nitrification) are well studied in  
58 these areas (Kalvelage et al., 2013; Lam et al., 2009; Jensen et al., 2011). The discovery of  $\text{NH}_4^+$ -  
59 oxidizing archaea (AOA) and their prominent roles in global nitrogen cycling in the OMZ have  
60 attracted great attention, because  $\text{NH}_4^+$  oxidation (nitrification) is the main process producing



61  $\text{NO}_3^-$  which then cause available N loss through denitrification and anammox (Ward et al., 2011;  
62 Hatzenpichler, 2012). In addition to nitrogen cycle studies, examination of the general  
63 organization and factors controlling the microbial community in the OMZ are still lacking (Ulloa  
64 et al., 2012). Pelagic prokaryotes in the OMZ do not seem fundamentally different from those  
65 present in oxygen-rich waters (Wright et al., 2012).

66         The basic mechanisms of oxygen depletion are similar in the permanent OMZ of the  
67 Open Ocean and seasonally hypoxic coastal areas. Both show a negative oxygen budget, despite  
68 the existence of large differences in water depth (several thousand meters versus < 100 m) and  
69 temporal scale (almost permanent versus seasonal). Comparison of the environments and biota of  
70 these two oxygen-minimum areas are needed, but few studies related to seasonal hypoxia and  
71 microbial ecology in coastal areas are available. Previous studies of coastal hypoxic areas reveal  
72 that decreased DO concentrations do not decrease microbial activity in the water column  
73 (Nogales et al., 2011; Crump et al., 2007). According to bacterial secondary production data,  
74 bacterial activity remains unchanged or even increases as hypoxia matures (Bastviken et al.,  
75 2001; Cole and Pace, 1995). However, bacterial production estimates based on leucine or  
76 thymidine incorporation may not represent total remineralization activity; rather, it is an index of  
77 the net growth of limited microbial groups (Tuominen, 1995). Further, changes in the microbial  
78 community in the sediment may differ from those in the water column; more dramatic changes  
79 are expected in the sediment because of the steep redox gradient and elevated  $\text{H}_2\text{S}$  accumulation  
80 under hypoxic conditions (Gundersen and Jorgensen 1990). The hypoxic conditions also have  
81 significant impacts on the biogeographical shift of sediment microbial community composition  
82 depending on the salinity and sediment characteristics (Dang et al., 2008). Most microbial  
83 sediment studies have focused on compositional changes, rather than adopting combined



84 approaches that monitor microbial activity and molecular community changes (Ye et al., 2016).  
85 Benthic and pelagic systems are coupled tightly in the shallow coastal environments where  
86 seasonal hypoxia occurs (Rowe, 2001). Comprehensive studies incorporating both quantitative  
87 (microbial activity) and qualitative (genetic diversity and composition) approaches are needed to  
88 improve understanding of microbial responses to hypoxia (Crump et al., 2007).

89 Sulfur cycling microorganisms dominate anoxic metabolism in the ocean and are  
90 involved in various oxidative or reductive processes (Jørgensen, 1982). Sulfur-oxidizing  
91 prokaryotes (SOP) use diverse electron acceptors, such as  $O_2$ ,  $NO_3^-$ ,  $Mn^{3+/4+}$  and  $Fe^{3+}$  and  
92 perform  $CO_2$  fixation (Mattes et al., 2013). However, sulfate-reducing prokaryotes (SRP) use  
93 sulfate as an electron acceptor and help degrade organic materials in low-oxygen zones  
94 (Jørgensen, 1982; Jørgensen and Postgate, 1982; Bowles et al., 2014). Specific 16S ribosomal  
95 RNA (rRNA) probes targeting specific genera of interest were developed to determine  
96 abundance of sulfur cycling prokaryotes in marine sediment (Ravenschlag et al., 2000; Gittel et  
97 al., 2008). This technique provides valuable genetic information, but the phylogenetic diversity  
98 of sulfur cycling prokaryotes complicates their detection (Stahl et al., 2002). The use of  
99 functional marker genes provides an alternative molecular approach. One such functional gene is  
100 *dissimilatory sulfite reductase*, which is the key enzyme of sulfate reduction and is present in  
101 genetically diverse sulfur cycling species, including Gram-positive and Gram-negative bacteria  
102 (Wagner et al., 1998; Kondo et al., 2004). However, the primer sets (for example DSR1F&4R)  
103 were restricted to SRP species, which is a major limitation, especially when the concomitant  
104 detection of both SRP and SOP organisms is required (Wagner et al., 1998). Another functional  
105 gene candidate is the *adenosine 5'-phosphosulfate (APS) reductase alpha subunit* gene (*aprA*).  
106 APS reductase consisting of an alpha (*aprA*) and beta (*aprB*) subunit is involved in dissimilatory



107 sulfate-reduction and converts APS into sulfite and adenosine monophosphate. PCR trials using  
108 primers for the *aprA* gene amplified both SRP and SOP species successfully in estuarine  
109 sediments and hydrothermal water, allowing detection of more diverse groups and improving  
110 understanding of the community structures of sulfur cycling prokaryotes (Meyer and Kuever,  
111 2007a; Meyer and Kuever, 2007b).

112           Jinhae Bay is a semi-enclosed bay on the south-eastern coast of South Korea. Massive  
113 industrialization and urbanization, started in the 1960s, has caused serious water-quality  
114 problems, including seasonal hypoxia every summer. Significant governmental efforts to reduce  
115 hypoxia since the 1980s have achieved only limited success (Lee et al., 2017). The development  
116 of seasonal hypoxia in coastal areas like Jinhae Bay may have a significant impact both directly  
117 and indirectly on the structure of microbial communities. However, the structure of the microbial  
118 community in Jinhae Bay under hypoxic conditions has not been studied in detail.

119           In this study, we investigated the dynamics of the microbial community with hypoxia  
120 development in Jinhae Bay to examine the following hypotheses: (a) the influences of hypoxia  
121 differ between water column and sediment (b) sulfur related microbes dominate microbial  
122 community changes during hypoxia development (c) various nitrogen dynamics in the permanent  
123 OMZ might also be important in coastal hypoxic zones like Jinhae Bay. Water-column  
124 characteristics were monitored to evaluate environmental changes. Oxygen demands were  
125 measured in both the water column (WOD) and sediment (SOD), to determine the correlation  
126 between oxygen depletion and microbial activity. Total remineralization activity was measured  
127 by membrane inlet mass spectrometer (MIMS) (An et al., 2001; Kana et al., 1994) to quantify  
128 DO changes for WOD and SOD. Temporal dynamics of  $\text{NO}_3^-$  and  $\text{NH}_4^+$  concentrations were  
129 measured to examine the effects of hypoxia on nitrogen cycling microorganisms. Relative



130 microbial abundance was measured using quantitative PCR (qPCR) with various primers,  
131 including those for bacterial and archaeal 16S rRNA genes. We also examined changes in the  
132 abundance and community structure of sulfur-cycling microbial groups using molecular  
133 techniques.

134

135

## 136 **2 Materials and methods**

### 137 **2.1 Site description and sample collection**

138 Dangdong Bay is a shallow (~13 m mean depth), semi-enclosed inner bay of Jinhae Bay in the  
139 southeastern part of the Korean Peninsula. The semi-diurnal, mean tidal range is 203 cm. Water  
140 exchange with the open ocean is limited in Jinhae Bay because it is surrounded by many small  
141 islands (Lee et al., 2017; Ministry of Oceans and Fisheries, 2015).

142 Vertical profiles of temperature and DO concentration were investigated weekly or  
143 biweekly from January–November 2015 using a Hydrolab multiprobe (Hydrolab® 4a) at the  
144 Dangdong Bay study site (Lee et al., 2017). Water samples were collected from the surface,  
145 middle, and bottom layers using a 5 L Niskin water sampler, and sediment cores were collected  
146 by scuba divers in five sampling periods (Fig. 1; S1(Solubility period), H2A, H2B, H3A, and  
147 H3B (Hypoxia periods)). Water samples for  $\text{NH}_4^+$  and  $\text{NO}_3^-$  measurement were filtered (25-mm  
148 GF/F filters; Whatman International, Maidstone, Kent, UK) and the filtrates transferred into 50-  
149 ml conical tubes and frozen until analysis. The concentrations of  $\text{NH}_4^+$  and  $\text{NO}_3^-$  were  
150 determined by standard methods using a spectrophotometer (Strickland and Parsons, 1972).

151 Water samples for WOD measurement were collected with Niskin bottles, and  
152 transferred into four 20-ml bottles (Wheaton Industries, Inc., Millville, NJ, USA).  $\text{ZnCl}_2$  (50%



153 [w/v]) was used to fix the samples in two bottles, and the other two were not fixed. DO  
154 concentration was measured using a MIMS system after 24–48 hrs of dark incubation at the *in*  
155 *situ* temperature (McCarthy et al., 2013).

156 For SOD measurement, eight intact sediment cores (internal diameter 8 cm; length 33  
157 cm) were collected by scuba divers (An and Joye, 2001) and pre-incubated with the overlying  
158 water for 12–24 h at *in situ* temperature to achieve equilibrium. After pre-incubation, the cores  
159 were closed with rubber stoppers, and duplicate cores were sacrificed at 0, 1, 2, and 24 h for DO  
160 measurement using MIMS. Oxygen concentration was quantified from the O<sub>2</sub>: Ar ratio (Kana et  
161 al., 1994; An et al., 2001). WOD ( $\mu\text{mol O}_2 \text{ l}^{-1} \text{ h}^{-1}$ ) obtained from the DO concentration  
162 difference between the fixed and unfixed samples. SOD ( $\text{mmol m}^{-2} \text{ d}^{-1}$ ) was calculated from the  
163 temporal DO concentration change considering the sediment core surface area.

164

## 165 **2.2 DNA Extraction**

166 Water samples for DNA extraction were collected from three different depths (top, middle, and  
167 bottom). Cells from 1 liter of each seawater sample were filtered through a polycarbonate filter  
168 with a pore size of 0.22  $\mu\text{m}$  (diameter: 25 mm; EMD Millipore Corp., Billerica, MA, USA),  
169 transferred into 35-mm diameter sterile Petri dishes, and kept at  $-20^\circ\text{C}$  until further processing in  
170 the laboratory. The filter paper containing the cells was folded in half using sterilized tweezers,  
171 and cut aseptically into two equal pieces. Each piece was inserted into a separate microcentrifuge  
172 tube and used for DNA extraction. DNA was extracted using a QIAamp<sup>®</sup> DNA Mini Kit (Qiagen,  
173 Hilden, Germany) according to the manufacturer's instructions, eluted with 100  $\mu\text{l}$  of double-  
174 distilled water, and kept at  $-80^\circ\text{C}$  until use. DNA was extracted from 0.4–0.5 g sediment using a  
175 FastDNA<sup>®</sup> SPIN KIT for Soil (MP Biomedicals, Santa Ana, CA, USA) according to the





176 manufacturer's protocol. DNA was eluted in a final volume of 50 µl of double-distilled water,  
177 and kept at –80°C until use. DNA quantity and quality were measured using a NanoDrop® 2000  
178 spectrophotometer (Thermo Fisher Scientific, Waltham, MA, USA).

179

### 180 **2.3 Polymerase chain reaction amplification**

181 Each PCR was performed in a 20 µl reaction volume using F-Star Taq DNA Polymerase  
182 (BioFact Co., Ltd., Daejeon, South Korea) following the manufacturer's instructions. Six  
183 different primers, comprising AprA-1-FW (5'-TGG CAG ATC ATG ATY MAY GG-3'), AprA-5-  
184 RV (5'-GCG CCA ACY GGR CCR TA-3'), Bac340 Forward (5'-TCC TAC GGG AGG CAG  
185 CAG T-3'), Bac515 Reverse (5'-CGT ATT ACC GCG GCT GCT GGC AC-3'), Arc915 Forward  
186 (5'-AGG AAT TGG CGG GGG AGC AC-3'), and Arc1059 Reverse (5'-GCC ATG CAC CWC  
187 CTC T-3'), were used in this study (Meyer and Kuever, 2007b; Nadkarni et al., 2002; Takai and  
188 Horikoshi, 2000; Yu et al., 2005). The PCR mixtures contained 10 µl of F-Star Taq mix, 2 µl of  
189 template, 1 µl of each forward and reverse primer (final concentration: 200 nM), and 6 µl of  
190 double-distilled water, yielding a final volume of 20 µl. The PCR cycle consisted of a 4-min  
191 denaturation step at 94°C, followed by 40 cycles of 94°C for 1 min, 48°C for 1 min, and 72°C  
192 for 2 min, and a final elongation step of 72°C for 10 min.

193

### 194 **2.4 Cloning and sequencing of adenosine 5'-phosphosulfate reductase alpha subunit genes**

195 The amplified products were viewed on 1% agarose gels using electrophoresis, and then purified  
196 using a HiGene™ Gel & PCR Purification System (BioFact Co., Ltd., South Korea) following  
197 the manufacturer's protocol. The purified amplicons were ligated into the T-Blunt™ vector, and  
198 transformed into T-Blunt™ Chemically Competent *Escherichia coli* Cells using a T-Blunt™



199 PCR Cloning Kit according to the manufacturer's instructions (SolGent Co., Ltd., Daejeon,  
200 South Korea). Colony PCR amplifications were performed with M13 reverse (–20) and forward  
201 (–20) primer sets, and clones with DNA inserts of the expected size were sent to the Bioneer  
202 Sequencing Service Center for sequencing (Bioneer, Daejeon, South Korea). Vector sequences  
203 were removed and edited using BioEdit software (Hall, 1999).

204

## 205 **2.5 Quantitative PCR analysis**

206 Quantitative PCR measurements of bacterial and archaeal 16S rRNA and *aprA* genes were  
207 conducted in triplicate on a Chromo4™ Real-Time PCR Detection System (Bio-Rad  
208 Laboratories, Inc., Hercules, CA, USA). DNA standards for bacterial and archaeal 16S rRNA  
209 genes were made from pure cultures of *E. coli* and *Sulfolobus acidocaldarius*, respectively. PCR  
210 amplification of 16S rRNA gene was performed and the products were cloned into the T-Blunt™  
211 vector, as described above. Plasmids containing an insert of the expected size were confirmed by  
212 sequence analysis, and purified further using a HiGene™ Plasmid Mini Prep Kit (BioFact Co.,  
213 Ltd.) following the manufacturer's protocol. Initial gene copy numbers of the extracted plasmids  
214 were calculated from the DNA concentrations, the length of the cloned gene fragments, and the  
215 mean weight of a base pair (660 g/mole). Serial dilution of the plasmids was performed to adjust  
216 the concentrations from  $1 \times 10^1$  to  $1 \times 10^9$  copies/μl. For the *aprA* gene standards, one *aprA*  
217 clone obtained from this study was selected, purified, and prepared as described above for  
218 bacterial and archaeal DNA standards. The concentration of the *aprA* clone was adjusted to be  
219 from  $1 \times 10^1$  to  $1 \times 10^7$  copies/μl.

220 The qPCR assay was performed as described previously (Purcell et al., 2014). Briefly,  
221 qPCR was performed using SYBR® green TOPreal™ qPCR 2X PreMIX (Enzynomics, Daejeon,



222 South Korea), and a primer concentration of 80 nM for both the bacterial and archaeal 16S rRNA  
223 genes and 200 nM for the *aprA* gene. The qPCR amplification conditions were as follows: 95°C  
224 for 5 min, and 40 cycles of 95°C for 1 min and 60°C for 30 s. A 2- $\mu$ l sample of DNA was used in  
225 each PCR reaction, which had a total volume of 20  $\mu$ l. Melting curve analyses were conducted  
226 after each assay to check PCR specificity. Coefficients of determination ( $R^2$ ) for standard curves  
227  $\geq 0.99$  and qPCR efficiencies ( $E$ )  $\geq 80\%$  were accepted.

228

## 229 2.6 Phylogenetic analysis

230 Nucleotide sequences were aligned and analyzed using the BioEdit program (Hall, 1999). After  
231 the vector sequences were removed, the nucleotide sequences were translated into amino-acid  
232 sequences, and clustered using ClustalW (Larkin et al., 2007) in BioEdit. The operational  
233 taxonomic units (OTUs) of the *aprA* gene were defined by a 90% or greater amino-acid sequence  
234 identity. Each *aprA* gene sequence was grouped into OTUs using the BLASTClust tool  
235 (<http://www.toolkit.tuebingen.mpg.de/blastclust>). A similarity search at the amino-acid level was  
236 performed against the NR database of the National Center for Biotechnology Information using  
237 BLASTP (<http://blast.be-md.ncbi.nlm.nih.gov/Blast.cgi>). Phylogenetic trees were calculated  
238 using the neighbor-joining method. A tree was drawn with a bootstrap analysis of 1,000  
239 replicates using the MEGA program (Tamura et al., 2013). Nucleotide sequences of the *aprA*  
240 clones obtained in this study were deposited in GenBank under the accession numbers from  
241 KY223831 to KY223998.

242

243

## 244 3 Results



### 245 **3.1 Development of hypoxia in Jinhae Bay**

246 The bottom-water DO concentration in Jinhae Bay showed a typical bowl-shaped pattern (An's  
247 bowl, Lee et al., 2017) with hypoxia occurring during the summer (Fig. 1). During the winter and  
248 spring (January–March; Period S1), the water column was well mixed, and thermal stratification  
249 was not observed (Figs. 1,2A). The water temperature difference between the surface and bottom  
250 water increased in April, and caused thermal stratification and pycnocline formation (Fig. 2A).  
251 The temperature difference between the surface and bottom water increased, and the pycnocline  
252 was strengthened during the summer (late May to August; Period H2; Fig. 1) (Fig. 2A). Seasonal  
253 salinity variation was low in Jinhae Bay, indicating limited fresh water inputs, and the influence  
254 of salinity on pycnocline formation was not important (Lee et al., 2017). During the summer  
255 (May 28–Aug 22; Period H3), hypoxic conditions occurred with low DO (16–92  $\mu\text{M O}_2$ ; Figs.  
256 1,2B). The DO level recovered when the thermocline disappeared in September (Period H4, Fig.  
257 1).

258

### 259 **3.2 Oxygen, $\text{NO}_3^-$ , and $\text{NH}_4^+$ profile changes**

260 The DO concentration showed distinct vertical profiles between normoxic (S1, H2, H4, and S5)  
261 and hypoxic (H3) conditions (Fig. 2A). Depth profiles for  $\text{NO}_3^-$  under normoxic conditions were  
262 vertically homogenous, although a peak in surface water was observed in Period H2. During  
263 hypoxia, however, the maximum concentration was observed in the middle and bottom water  
264 (Fig. 2C).  $\text{NH}_4^+$  showed similar temporal variations to  $\text{NO}_3^-$  (Fig. 2D). The depth profile was  
265 vertically homogeneous during normoxia. Accumulation of  $\text{NH}_4^+$  in the bottom water was clear,  
266 with near detection limit concentrations in surface waters during hypoxia (Fig. 2D). In this  
267 period, the peak depth of  $\text{NO}_3^-$  tended to be shallower (7–12 m) than that of  $\text{NH}_4^+$  (>12 m; Fig.



268 2D).

269

### 270 **3.3 Oxygen demand in the water column and sediment**

271 WOD and SOD represent the rates of bacterial respiration and organic matter degradation. WOD  
272 varied from 0.1–0.5  $\mu\text{mol l}^{-1} \text{h}^{-1}$  (Fig. 3A). Bottom WOD increased with water temperature ( $r^2 =$   
273 0.99). SOD ranged from 2.4–23.5  $\text{mmol m}^{-2} \text{d}^{-1}$  (Fig. 3B). SOD tended to increase in early  
274 stages of hypoxia (H2A and H2B) and decreased with mature hypoxia (H3B; Fig. 3B). SOD was  
275 sensitive to the DO concentration of the bottom water and approached zero during hypoxia.  
276 Unlike WOD, SOD did not show a good correlation with water temperature.

277

### 278 **3.4 Quantitative PCR analysis**

279 qPCR for the bacterial and archaeal 16S rRNA and *aprA* genes in 20 samples revealed both  
280 spatial and temporal variations (Fig. 4). Comparison of qPCR results from water samples showed  
281 that the abundance of bacterial 16S rRNA genes was the lowest in bottom water, regardless of  
282 the sampling date. However, the abundance of archaeal 16S rRNA genes were the highest in  
283 middle water samples, implying that bacterial and archaeal groups respond differently to spatial  
284 variations. Increased copy numbers of the *aprA* gene were detected in bottom water at most  
285 stages except S1, indicating that most sulfur cycling prokaryotes was present in the bottom water.  
286 The relative abundance was measured with the percentage of *aprA* genes in relation to total  
287 prokaryote 16S rRNA genes. The percentage of *aprA* to the total prokaryote 16S rRNA gene in  
288 surface and mid-depth waters ranged from 0.04%–0.84% versus 5.35%–11.09% in bottom  
289 waters, showing that the relative abundance of *aprA* increased significantly with depth (t-test,  
290  $p < 0.01$ ). In sediment, higher copy numbers were observed for all genes, as expected. In addition,



291 the percentage of *aprA* to bacterial 16S rRNA gene ranged from 16.32%–44.76% in sediment  
292 samples, showing that sulfur cycling prokaryotes were more important in sediments than in the  
293 water column of Jinhae Bay.

294 In addition to spatial variations, changes in abundance associated with environmental  
295 conditions, especially hypoxia development, were examined using qPCR. No significant trends  
296 in the copy numbers of the three genes were observed in all water samples, except for a slight  
297 increase in the abundance of the archaeal 16S rRNA gene in the middle water column layer with  
298 hypoxia development (Fig. 4B). In addition, the abundance of the *aprA* gene relative to total  
299 bacteria was variable with oxygen depletion. For examples, water samples collected in Period S1  
300 ranged from 0.16–10.74%, whereas those water samples collected in Period H3B ranged from  
301 0.09%–6.86%. However, in the sediment, clear correlations between oxygen depletion and  
302 changes in microbial community abundance were observed. The total abundances of all three  
303 genes decreased with hypoxia development (Fig. 4D). In addition, the relative abundances of the  
304 *aprA* gene to total prokaryotes also significantly decreased from 14.9% to 5.2%.

305

### 306 **3.5 Sequence analysis of the adenosine 5'-phosphosulfate reductase alpha subunit gene**

307 PCR trials targeting a region of the *aprA* gene about 390 base pairs in size were successful in all  
308 samples, and the products were used for further cloning experiments (data not shown). Cloning  
309 and sequence analysis of the amplicons confirmed the detection of the *aprA* gene. From the 20  
310 different environmental samples, comprising five sediment and 15 water samples, a total of 168  
311 *aprA* clones were sequenced. Among them, 66 originated from various depths in the water  
312 column, and 102 were obtained from the sediment. Using the 90% amino-acid identities, all 168  
313 *aprA* sequences were grouped into 33 distinct OTUs. Comparison of the number of OTUs with



314 respect to the number of clones revealed that similar ratios (13–30%) of water and sediment  
315 clones were grouped into OTUs. Nine OTUs among the 66 water-derived clones (13%) were  
316 identified, whereas 31 OTUs among the 102 sediment-derived clones (30%) were detected. The  
317 ratios were variable, ranging from 21–40%, when the OTU numbers with respect to the clone  
318 numbers were compared in each layer, including the surface, middle, and bottom water and  
319 sediment. The smallest ratio was observed in the top layer of the water clones. Only seven OTUs  
320 were observed among the 32 sequenced clones (21%), indicating that most similar *aprA* clones  
321 were obtained from the surface water.

322         Sequence analysis revealed that the most commonly detected group was OTU 13. About  
323 29% of the *aprA* sequences (50/168) belonged to this group. Phylogenetic analysis indicated that  
324 OTU 13 was affiliated to SOP Lineage I, which showed the highest amino-acid-sequence identity  
325 (92%) to Gamma proteobacterium SCGC (Table 1). The second largest group, OTU 21,  
326 consisting of 35 clones (20% of *aprA* clones), was also designated as SOP Lineage I. Although  
327 two large OTUs belonged to the same functional group, most clones in OTU 13 were derived  
328 from the water (45/50), especially the surface layer (24/42), whereas the clones in OTU 21  
329 mainly originated from sediment (27/35). In addition, SOP Lineage I consisted of three other  
330 OTUs: 4, 9, and 28 (Fig. 5). About 60% (101/168) of the clones analyzed in this study fell into  
331 this group, implying that this is the most common functional group in Jinhae Bay. Comparison of  
332 the sequence similarity revealed that about 10% (17/168) of the *aprA* clones showed similarity to  
333 another sulfur-oxidizing functional group: SOP Lineage II. Most of these clones were grouped  
334 into OTU 3 (94%, 16/17), and were mainly obtained from sediment (88%, 15/17). In addition to  
335 OTU 3, OUT 29 was affiliated with the SOP Lineage II group and showed amino-acid-sequence  
336 identities (67–97%) with various organisms, such as *Candidatus pelagibacter ubique*, *Olavius*



337 *algarvensis* gamma 1 endosymbiont isolates, and bacterial endosymbionts of *Lucinoma* aff.  
338 *kazani*.

339 Nineteen *aprA* OTUs were designated Gram-positive sulfate-reducing bacteria (SRB)  
340 and comprised about 14% of the total *aprA* clones (24/168; Table 1). Considering both clone and  
341 OTU numbers, the highest OTU numbers were observed in this group. Nine-teen OTUs were  
342 detected among 24 *aprA* clones, indicating a large range of genetic diversity. Most clones (23/24)  
343 were derived from the sediment, in contrast to the SOP Lineage I group. A BLASTP search  
344 showed various amino-acid identities, ranging from 58–97%, to known SRB species, including  
345 *Desulfotomaculum kuznetsovii* (66–88%), *Desulfomonile tiedjei* (62–85%), and *Nitrospira*  
346 *bacteria* (74–97%; Fig. 5). Seven *aprA* OTUs (2, 5, 6, 11, 16, 25 and 27) resembled other SRB  
347 groups (Table 1). Six OTUs (2, 5, 6, 11, 16 and 27) were grouped as Deltaproteobacterial SRB  
348 species, whereas the last OTU 25 was attributed to the thermophilic SRB group. Most clones  
349 (80%, 21/26) of these seven OTUs originated from the sediment as observed for the Gram-  
350 positive SRB group. One thermophilic OTU displayed the highest amino-acid identity (58–76%)  
351 to *Thermodesulfovibrio islandicus*, whereas the other six OTUs revealed various amino-acid  
352 identities (67–97%) to known SRB species, including *Desulfonatronovibrio hydrogenovorans*  
353 (69–76%), *Desulfofustis glycolicus* (73–97%), and *Desulfobacter curvatus* (67–95%).

354 Occurrences of *aprA* gene were compared to examine the effects of hypoxia  
355 development on the diversity of sulfur cycling microorganisms, Sulfur-oxidizing *aprA* sequences,  
356 especially from Lineage I group, dominated all water samples (Fig. 6). About 83% (20/24) of the  
357 clones originating from water samples collected in Period S1 were grouped into either sulfur-  
358 oxidizing Lineages I or II, and similarly, all clones originating from water samples collected in  
359 Period H2B were classified as the same functional SOP groups of S1 clones. In contrast to the





360 presence of similar functional groups in water samples, changes in *aprA* functional groups with  
361 hypoxia development were observed. In sediment collected in Period S1, the sulfur-oxidizing  
362 groups SOP I and II were dominant. A total of 82% of clones (19/23) belonged to these two  
363 groups. However, in sediment collected in Period H3B, *aprA* clones related to sulfur oxidizers  
364 decreased to 29% (7/24), whereas clones grouped as sulfate reducers increased to 70% (17/24;  
365 Fig. 6).

366

367

#### 368 **4 Discussions and conclusions**

##### 369 **Microbial abundance and activity changes**

370 Microbial communities are complex in nature, and their structures and functions change rapidly  
371 in response to various environmental factors (Fuhrman et al., 2015). However, the major factors  
372 affecting the structural dynamics of microbial communities differ depending on time and space  
373 (Dang and Chen, 2017). The main purposes of this study were to understand the microbial  
374 community responses to suboxic/anoxic conditions, such as 1) how the amount of microbial  
375 activity are affected (quantitative aspects) and 2) how the structure of the microbial community  
376 are changed (qualitative aspects). In our study, an overall decrease in bacteria and archaea in the  
377 sediment occurred with developing hypoxic conditions, indicating that oxygen depletion is a  
378 main driver of change in microbial communities. In addition to oxygen concentration, other  
379 environmental factors, such as temperature, had a direct impact on microbial communities. For  
380 example, SOD increased in the early stage of hypoxia (Period H2A and H2B, Fig. 3B) compared  
381 with Period S1, probably due to favorable water temperature. At these H2 stages, DO levels  
382 decreased but were high enough for aerobic respiration. However, at hypoxia stage H3B, despite



383 the highest water temperature, SOD was significantly decreased, suggesting that low oxygen  
384 concentration is the major factor leading to changes in sediment microbial communities

385 Unlike SOD, WOD gradually increased from stages S1 to H3B, indicating that oxygen  
386 depletion may not affect microbial communities in the water as significantly as those in the  
387 sediment (Fig. 3A). Instead, positive correlations between WOD and temperature from stages S1  
388 to H2B indicate that temperature affected microbial activities in the water more than oxygen  
389 depletion. Likewise, Crump et al. (2007) also reported that microbial activity among water-  
390 column bacteria was unaffected by oxic–anoxic transitions, although compositional and  
391 functional group changes occurred under mature hypoxia (Crump et al., 2007; Nogales et al.,  
392 2011). Interestingly, Crump et al. (2007) were aware of the importance of the benthic microbial  
393 community in shallow coastal waters like Chesapeake Bay (USA); however, the clear decrease in  
394 bacterial activity in the sediment with hypoxia development observed in this study was not  
395 foreseen in their study. In addition to temporal effects on oxygen concentration, our WOD data  
396 displayed an increase in bottom water and a decrease in both surface and middle water during  
397 hypoxia (H3B), revealing that oxygen concentration may lead to spatial variations in microbial  
398 communities of water column (Fig. 3A). In addition, the detection of a relatively high WOD in  
399 the bottom water in Period H3B was quite unexpected because it is contradictory to the result  
400 observed in the sediment at the same stage (Fig. 3). From our data, we conclude that microbial  
401 aerobic respiration continues under hypoxic conditions in the water, but not in the sediment. The  
402 flux of oxygen through eddy diffusion from the surface water column appeared to support  
403 aerobic respiration, even though DO concentration was quite low at this stage (< 20% saturation,  
404 Fig. 1). Substantial transport of oxygen into the hypoxic zone could occur during the Period H3,  
405 although increase of DO was not observed due to the high oxygen consumption rates (Lee et al.,



406 2017).

407 Another interesting result was the positive correlation between microbial activity and  
408 abundance. Many reports have shown a positive correlation between SOD and DO concentration;  
409 but the mechanisms of the correlations are not clear (Rowe, 2001; Hetland and DiMarco, 2008;  
410 Murrell and Lehrter, 2011). It is possible that the decreased SOD in low-DO conditions can be  
411 attributed to either a reduction in the aerobic microbial community or a transition to less efficient  
412 anaerobic metabolism pathways (Rowe 2001; An et al., 2001; Dang and Jiao 2014). However,  
413 under mature hypoxic conditions, the microbial communities may have already been adapted to  
414 anaerobic respirations using alternative electron acceptors such as  $\text{Mn}^{3+/4+}$ ,  $\text{Fe}^{3+}$  and  $\text{SO}_4^{2-}$  (Dang  
415 and Jiao, 2014). In such cases, the decrease of SOD may not necessarily mean the decreased  
416 microbial respiration activity. In our study, bacteria abundances (qPCR) decreased with  
417 decreasing microbial activity (SOD) and vice versa, revealing a positive correlation across  
418 sampling site, even though the overall activity trend in the sediment was opposite to that in the  
419 water (Fig. 3). Considering both SOD and qPCR data together, we speculate that perhaps the  
420 decreased SOD with hypoxia development is caused by a reduction in total microbial abundance  
421 more than a switch to less efficient anaerobic metabolism. However, in water, both WOD and  
422 microbial abundance correlated with temperature changes, but not to hypoxia development,  
423 implying no significant effects of hypoxia on either microbial activity or abundance in water.

424

#### 425 **Nitrogen-cycling microorganisms**

426 In addition to variations in the total microbial community, bacterial and archaeal groups  
427 responded differently to hypoxia development (Fig. 4). Recently, Hewson et al. (2014) showed  
428 increased archaeal activity occurred as hypoxia matured in Chesapeake Bay (Hewson et al.,



429 2014). They proposed that increased  $\text{NH}_4^+$  availability under low DO conditions provided  
430 potential substrates for chemoautotrophic archaeal, such as AOA (mostly *Nitrospumilus marinus*)  
431 and caused archaeal increases. Considering both the ubiquitous nature of AOA and our vertical  
432 nutrient profile data together, the variations in archaeal abundance in water column with hypoxia  
433 development may possibly be caused by AOA in the water column (Berg et al., 2015). During  
434 hypoxia, the  $\text{NO}_3^-$  profile peaked at the middle depth (7–12 m), whereas  $\text{NH}_4^+$  concentrations  
435 were low at the middle depth, compared with the bottom water, implying active nitrification  
436 activity (Figs. 2C,D).

437         The temporal variation in archaea at each water depth indicates that AOA could be  
438 related to this pattern. During the early stage of hypoxia (H2A), archaea increased in surface  
439 water when enough  $\text{NH}_4^+$  was present (Figs. 2D,3A). However, they decreased abruptly from  
440 H2B when  $\text{NH}_4^+$  was exhausted, because the intensified stratification blocked the supply of  
441 abundant  $\text{NH}_4^+$  from the bottom water (Figs. 2A,D). At this stage, nitrification activity could be  
442 limited by low  $\text{NH}_4^+$  availability, despite the high DO concentration. Similarly, a decrease in  
443 archaea with hypoxia development was observed in the bottom water (Fig. 4C). However, the  
444 reason for this decrease may differ from that of the surface water. In the bottom water, we  
445 assumed that sufficient  $\text{NH}_4^+$  was present, but not oxygen, because of the strong stratification  
446 and hypoxia (Figs. 2B,D). Reduced export of  $\text{NH}_4^+$  can be expected with strong stratification  
447 (Lee et al., 2017). A high  $\text{H}_2\text{S}$  concentration at the bottom can also inhibit nitrification, although  
448 AOA seem to be less sensitive to  $\text{H}_2\text{S}$  toxicity than  $\text{NH}_4^+$ -oxidizing bacteria (AOB) (Joye and  
449 Hollibaugh, 1995; Berg et al., 2015). Nonetheless, the decrease in archaeal abundance in the  
450 bottom water may have resulted from decreased nitrification activity caused by low oxygen  
451 concentration with hypoxia, rather than a shortage of  $\text{NH}_4^+$ . Because the middle water has



452 frequent chances to develop favorable conditions for nitrification such as high availability of  
453 both  $\text{NH}_4^+$  and oxygen, relatively high nitrification activity is expected. Interestingly, in our  
454 study, the overall proportion of archaea (2–30%) tended to be higher in the middle water than in  
455 surface (0.1–2%) or bottom (2–50%) waters. Archaeal abundance gradually increased as the  
456 hypoxia matured, possibly supporting our hypothesis of a close relationship between nitrification  
457 activity and archaeal abundance in Jinhae Bay.

458 Our results demonstrate that seasonal hypoxia shows analogous microbial dynamics to  
459 permanent OMZ's despite the size difference (15 m versus ~3000 m water depth) as  
460 hypothesized. DO and DIN profiles observed in this study suggested that optimal conditions for  
461 AOA activity could be formed in the middle depth water. Similarly, active transcripts (up to 20%  
462 of all protein coding) of the *amoA* gene of AOA belonging to the phylum Thaumarchaeota  
463 occurred in the upper boundary of the OMZ, where optimal conditions for nitrification (high DO  
464 supply from surface water and high  $\text{NH}_4^+$  supply from bottom water) existed (Stewart et al.,  
465 2012). High abundance of archaeal *amoA* genes were evident in the upper boundary of almost all  
466 OMZs including ETNP, ESP, Black Sea, Gulf of California, and Baltic Sea (Ulloa et al., 2012).  
467 Unlike open oceans, however, the depth of optimal nitrification may quite vary as the pycnocline  
468 weakens or strengthens depending on the tide and weather conditions in a shallow estuary like  
469 Jinhae Bay (Lee et al., 2017). More detailed future studies, related to the various nitrogen  
470 processes such as denitrification, anammox, and DNRA under hypoxic condition, are definitely  
471 required in coastal regions because they are less studied compared to the permanent OMZ region  
472 (Abell et al., 2011; Ward et al., 2013). Moreover, the studies related to the nutrient-replete  
473 conditions and intensive interactions with sediment are also important to understand the complex  
474 nitrogen dynamics in coastal areas (McCarthy et al., 2013).



475           The abundance of sediment bacteria decreased as hypoxia developed (Fig. 4D), which is  
476 consistent with the total microbial abundance and SOD results (Fig. 3B). We believe that the  
477 succession from aerobic to anaerobic metabolism was not established, and the aerobic bacteria  
478 might be responsible for the decrease. In contrast to the bacteria, sediment archaea were less  
479 affected by hypoxia and dominated in Periods H2A, H3A, and H3B as hypoxia developed (Fig.  
480 4D). Swan et al. (2000) reported that archaea appeared to be more tolerant to low oxygen than  
481 bacteria in sediment (Swan et al., 2010). In this study, the increasing archaeal abundance with  
482 hypoxia development was observed in the middle water as well as in the sediment (Fig. 4B).  
483 Although similar trends were observed in both middle water and sediment; the reasons for  
484 increasing archaeal populations could differ. As discussed above, AOA seems to be responsible  
485 for the archaea abundance variation in the middle water. Abell et al. (2011) reported lower DO  
486 sensitivity of AOA compared to AOB (ammonium oxidizing bacteria) in an *amoA* transcription  
487 study (Abell et al., 2011). Therefore, the AOA seems to be responsible for the increased archaeal  
488 importance with middle water hypoxia development. In sediment, however, the oxygen  
489 availability is very low and should limit AOA activity during hypoxia, so the increase of archaeal  
490 importance in the hypoxia cannot be explained with AOA. A methanogenesis processing archaeal  
491 group seems to be another explanation, considering the organic-rich conditions of Jinhae Bay  
492 (Munson et al., 1997). Although methanogens are less competitive than SRP under anoxic  
493 conditions, methanogenic archaea successfully co-occur in certain conditions if noncompetitive  
494 substrates, including methanol, methylamine, and methionine are available (Munson et al., 1997).  
495 More future studies addressing how the relative dominance of SRP vs. archaea occurs in Jinhae  
496 Bay may be interesting.

497

498 **Sulfur-cycling microorganisms**

499 Sequence analysis indicated that large numbers of clones were SOPs; however, most of these  
500 SOP-related OTUs were not assigned clearly into specific SOP species or genera (Watanabe et al.,  
501 2013). Similar problems were faced in other studies, because only limited numbers of *aprA*  
502 sequence data are available and low bootstrap values were present in the SOP lineages. Although  
503 each OTU was not classified into a specific species, the most common one, OTU 13, was  
504 affiliated to the *aprA* Lineage I cluster, which includes bacterial species such as the  
505 chemolithoautotrophic betaproteobacterium *Thiobacillus thioparus* and the phototrophic  
506 gammaproteobacterium *Thiocapsa rosea*. The second most common OTU, 21, was also affiliated  
507 with the *aprA* Lineage I cluster, suggesting that the main groups of SOP present in Jinhae Bay  
508 belong to *aprA* Lineage I. Purcell et al. (2014) also showed that most sulfur oxidizers in the  
509 subglacial Lake Whillans (Antarctica) belonged to the *aprA* Lineage I (Purcell et al., 2014).  
510 However, all clones from this subglacial lake originated from the sediment, whereas our clones  
511 derived from both the water and the sediment. Most sulfur-oxidizer clones in the water column  
512 belonged to OTU 13, demonstrating a close relationship to *aprA* Lineage I. In contrast to the  
513 existence of one major group of sulfur oxidizers in water, at least three different groups,  
514 including OTUs 3, 4, and 21, were present in the sediment. These clones were affiliated to either  
515 *aprA* Lineages I or II. Our results suggest that more genetically diverse groups of sulfur oxidizers  
516 are present in the sediment of Jinhae Bay, although more comprehensive studies with enough  
517 clone library sizes might be helpful to sharpen our data.

518         Diverse sulfate-reducing *aprA* genes were identified in the current study and many  
519 clones were affiliated to the family *Desulfobacteraceae*. Reportedly, *Desulfobacteraceae* is one  
520 of the most abundant SRB groups in the subsea floor environment (Foti et al., 2007; Kjeldsen et



521 al., 2007; Kuever, 2014). In addition to the heterogenetic metabolism, members of the  
522 *Desulfobacteraceae* family can grow chemolithoautotrophically using hydrogen or by  
523 fermentation, iron reduction, or the disproportionation of inorganic sulfur compounds. Other  
524 *aprA* gene groups such as *Desulfotomaculum* and *Desulfobulbaceae* occurred in Jinhae Bay and  
525 can oxidize various organic substances using sulfur compounds as the electron acceptor.

526 Both qPCR and studies of genetic diversity demonstrated that *aprA*-related  
527 microorganisms were affected by hypoxia development, but they responded differently  
528 depending on sampling site and their functional groups. In the water column, SOPs were  
529 dominant, and no significant changes were observed in either their abundance or diversity (Fig.  
530 6). However, in the sediment, more genetically diverse SRPs were detected with hypoxia  
531 development, suggesting that hypoxia causes favorable conditions for SRPs in the sediment, but  
532 not in the water. OTUs 13 and 21, belonging to SOP Lineage I, occurred frequently both in the  
533 water column and the sediment. However, sensitivity to oxygen concentration differs between  
534 these OTUs. When hypoxia matured in Period H3B, OTU 21 still appeared in the sediment,  
535 whereas OTU 13 was absent in both the sediment and the bottom water (although OTU 13 still  
536 appeared in the top and middle water, where oxygen levels remained high). Therefore, OTU 13  
537 may represent a candidate instigator of the reduced *aprA* abundance evident in the qPCR analysis  
538 of sediment samples (Fig. 4D). Most sulfur reducers found increasingly during hypoxic stages  
539 were SRB of the class *Deltaproteobacteria* or Gram-positive SRB of the genus  
540 *Desulfotomaculum*. *Deltaproteobacteria*-SRB (D-SRB) groups were detected throughout the  
541 seasons, whereas different OTUs belonging to Gram-positive-SRB (G-SRB) mostly present in  
542 the sediment (except OTU 1 of top layer in stage S1) and showed distinctive occurrences in each  
543 stage (a “SRB succession”; Fig. 6D). The SRB succession implies that the various G-SRB OTUs





544 are sensitive to a small DO change. The number of OTUs during the SRB succession tended to  
545 increase as hypoxia matured (From H2B to H3B). At pre-hypoxia stage H2A, diverse and  
546 distinctive G-SRB OTUs were observed. This result was not expected because DO should be  
547 relatively high compared to the H3 states. Other environmental factors, including temperature,  
548 salinity, and organic compounds may be important for the SRB succession (Wright et al., 2012).  
549 The SRB succession might also be the results of interactions with the cryptic sulfur cycle  
550 (autotrophic denitrification), which could enhance the SRB activity in certain microenvironments  
551 (Canfield et al., 2010; Shao et al., 2010; Dang and Lovell, 2016). More detailed studies are  
552 certainly necessary to define and explain how SRB succession occurs, but our results  
553 demonstrate distinctive responses of sediment microbes to hypoxia in terms of microbial  
554 community structure.

555

#### 556 **FUNDING**

557 This project was supported by Korea Ministry of Environment as “Climate Change  
558 Correspondence Program”.

559

#### 560 **ACKNOWLEDGMENTS**

561 The authors want to thank Dr. Lee, J.Y. and Ms. Huh, N. for her help during field sampling and  
562 editing. We also thank Dr. Wayne Gardner and Dr. Mark McCarthy for helpful suggestions.

563



564 **References**

565

566 Abell, G. C., Banks, J., Ross, D. J., Keane, J. P., Robert, S. S., Reville, A. T., et al.: Effects of  
567 estuarine sediment hypoxia on nitrogen fluxes and ammonia oxidizer gene transcription,  
568 *FEMS Microbiol. Ecol.*, 75, 111–122, doi: 10.1111/j.1574-6941.2010.00988.x, 2011.

569 An, S., and Joye, S. B.: Enhancement of coupled nitrification denitrification by benthic  
570 photosynthesis in shallow estuarine sediments, *Limnol. Oceanogr.*, 46, 62–74, doi:  
571 10.4319/lo.2001.46.1.0062, 2001.

572 An, S., Gardner, W. S., and Kana, T.: Simultaneous measurement of denitrification and nitrogen  
573 fixation using isotope pairing with membrane inlet mass spectrometry analysis, *Appl.*  
574 *Environ. Microbiol.*, 67, 1171–1178, doi: 10.1128/AEM.67.3.1171-1178.2001, 2001.

575 Bastviken, D., and Tranvik, L.: The leucine incorporation method estimates bacterial growth  
576 equally well in both oxic and anoxic lake waters, *Appl. Environ. Microbiol.*, 67, 2916–2921,  
577 doi: 10.1128/AEM.67.7.2916-2921.2001, 2001.

578 Berg, C., Vandieken, V., Thamdrup, B. and Jürgens, K.: Significance of archaeal nitrification in  
579 hypoxic waters of the Baltic Sea, *ISME J.*, 9(6), 1319-1332, doi: 10.1038/ismej.2014.218,  
580 2015.

581 Bowles, M. W., Mogollón, J. M., Kasten, S., Zabel, M., and Hinrichs, K. U.: Global rates of  
582 marine sulfate reduction and implications for sub-sea-floor metabolic activities, *Science*, 344,  
583 889–891, doi: 10.1126/science.1249213, 2014.

584 Cole, J. J., and Pace, M. L.: Bacterial secondary production in oxic and anoxic fresh-waters,  
585 *Limnol. Oceanogr.*, 40, 1019–1027, doi: 10.4319/lo.1995.40.6.1019, 1995.

586 Crump, B. C., Peranteau, C., Beckingham, B., and Cornwell, J. C.: Respiratory succession and



- 587 community succession of bacterioplankton in seasonally anoxic estuarine waters, Appl.  
588 Environ. Microbiol., 73, 6802–6810, doi: 10.1128/AEM.00648-07, 2007.
- 589 Dang, H., Zhang, X., Sun, J., Li, T., Zhang, Z., and Yang, G.: Diversity and spatial distribution  
590 of sediment ammonia-oxidizing crenarchaeota in response to estuarine and environmental  
591 gradients in the Changjiang Estuary and East China Sea, Microbiol., 154, 2084–2095, doi:  
592 10.1099/mic.0.2007/013581-0, 2008.
- 593 Dang, H., Chen, R., Wang, L., Shao, S., Dai, L., Ye, Y., Guo, L., Huang, G., and Klotz, MG.:  
594 Molecular characterization of putative biocorroding microbiota with a novel niche detection  
595 of *Epsilon*- and *Zetaproteobacteria* in Pacific Ocean coastal waters, Environ. Microbiol., 13,  
596 3059-3074, doi: 10.1111/j.1462-2920.2011.02583.x, 2011.
- 597 Dang, H. and N., Jiao.: Perspectives on the microbial carbon pump with special reference to  
598 microbial respiration and ecosystem efficiency in large estuarine systems,  
599 Biogeosciences, 11, 3887-3898, doi: 10.5194/bg-11-3887-2014, 2014.
- 600 Dang, H., and C.R. Lowell.: Microbial surface colonization and biofilm development in marine  
601 environments, Microbiol. Mol. Biol. Rev., 80, 91–138, doi: 10.1128/MMBR.00037-15,  
602 2016.
- 603 Dang H and C.A. Chen.: Ecological energetic perspectives on responses of nitrogen-  
604 transforming chemolithoautotrophic microbiota to changes in the marine environment, Front  
605 Microbiol., 8, 1246., doi: 10.3389/fmicb.2017.01246, 2017.
- 606 Diaz, R. J., and Rosenberg, R.: Spreading dead zones and consequences for marine ecosystems,  
607 Science, 3215891, 926–929, doi: 10.1126/science.1156401, 2008.
- 608 Foti, M., Sorokin, D. Y., Lomans, B., Mussman, M., Zacharova, E. E., Pimenov, N. V., et al.:  
609 Diversity, activity and abundance of sulfate-reducing bacteria in saline and hypersaline soda



- 610 Lakes, *Appl. Environ. Microbiol.*, 73, 2093–2100, doi: 10.1128/AEM.02622-06, 2007.
- 611 Fuhrman, J. A., Cram, J. A., and Needham, D. M.: Marine microbial community dynamics and  
612 their ecological interpretation, *Nat. Rev. Microbiol.*, 13, 133–146, doi: 10.1038/nrmicro3417,  
613 2015.
- 614 Gittel, A., Musmann, M., Sass, H., Cypionka, H., and Konneke, M.: Identity and abundance of  
615 active sulfate-reducing bacteria in deep tidal flat sediments determined by directed  
616 cultivation and CARD-FISH analysis, *Environ. Microbiol.*, 10, 2645–2658, doi:  
617 10.1111/j.1462-2920.2008.01686.x, 2008.
- 618 Gundersen, J. K. and B. B. Jørgensen.: Microstructure of diffusive boundary layers and the  
619 oxygen uptake of the sea floor, *Nature*, 345, 604–607, 1990.
- 620 Hall, T. A.: BioEdit: A user-friendly biological sequence alignment editor and analysis program  
621 for Windows 95/98/NT, *Nucleic Acids. Symp. Ser.*, 41, 95–98, doi: 10.1021/bk-1999-  
622 0734.ch008, 1999.
- 623 Hatzenpichler, R.: Diversity, physiology, and niche differentiation of ammonia-oxidizing  
624 archaeal, *Appl. Environ. Microbiol.*, 78, 7501–7510, doi: 10.1128/AEM.01960-12, 2012.
- 625 Hetland, R., and DiMarco, S.: How does the character of oxygen demand control the structure of  
626 hypoxia on the Texas-Louisiana continental shelf, *J. Mar. Syst.*, 70, 49–62, doi:  
627 10.1016/j.jmarsys.2007.03.002, 2008.
- 628 Hewson, I., Eggleston, E. M., Doherty, M., Lee, D. Y., Owens, M., Shapleigh, J. P. et al.:  
629 Metatranscriptomic analyses of plankton communities inhabiting surface and subpycnocline  
630 waters of the Chesapeake Bay during oxic-anoxic-oxic transitions, *Appl. Environ. Microbiol.*,  
631 80, 328–338, doi: 10.1128/AEM.02680-13, 2014.



- 632 Jensen, M. M., Lam, P., Revsbech, N. P., Nagel, B., Gaye, B., Jetten, M. S. et al.: Intensive  
633 nitrogen loss over the Omani Shelf due to anammox coupled with dissimilatory nitrite  
634 reduction to ammonium, *ISME J.*, 5, 1660–1670, doi: 10.1038/ismej.2011.44, 2011.
- 635 Joye, S. B., and Hollibaugh, J. T.: Sulfide inhibition of nitrification influences nitrogen  
636 regeneration in sediments, *Science*, 270, 623–625, doi: 10.1126/science.270.5236.623, 1995.
- 637 Jørgensen, B. B.: Mineralization of organic matter in the sea bed—the role of sulfate reduction,  
638 *Nature*, 296, 643–645, doi:10.1038/296643a0, 1982.
- 639 Jørgensen, B. B., and Postgate, J. R.: Ecology of the bacteria of the Sulphur cycle with special  
640 reference to anoxic-oxic interface environments and discussion, *Philos. Trans. R. Soc. Lond.*  
641 *B. Biol. Sci.*, 298, 543–561, doi: 10.1098/rstb.1982.0096, 1982.
- 642 Kalvelage, T., Lavik, G., Lam, P., Contreras, S., Arteaga, L., Löscher, C. R. et al.: Nitrogen  
643 cycling driven by organic matter export in the South Pacific oxygen minimum zone, *Nature*  
644 *Geosci.*, 6, 228–234, doi: 10.1038/ngeo1739, 2013.
- 645 Kana, T. M., Darkangelo, C., Hunt, M. D., Oldham, J. B., Bennett, G. E., and Cornwell, J. C.:  
646 Membrane inlet mass spectrometer for rapid high-precision determination of N<sub>2</sub>, O<sub>2</sub>, and Ar  
647 in environmental water samples, *Anal. Chem.*, 66, 4166–4170, doi: 10.1021/ac00095a009,  
648 1994.
- 649 Kjeldsen, K. U., Loy, A., Jakobsen, T. F., Thomsen, T. R., Wagner, M., and Ingvorsen, K.:  
650 Diversity of sulfate-reducing bacteria from an extreme hypersaline sediment, Great Salt Lake  
651 (Utah), *FEMS Microbiol. Ecol.*, 60, 287–298, doi: 10.1111/j.1574-6941.2007.00288.x, 2007.
- 652 Kondo, R., Nedwell, D. B., Purdy, K. J., de Queiroz Silva, S.: Detection and enumeration of  
653 sulfate-reducing bacteria in estuarine sediments by competitive PCR, *Geomicrobiol.*, 21,  
654 145–157, doi: 10.1080/01490450490275307, 2004.



- 655 Kuever, J.: “The Family Desulfobacteraceae,” in *The Prokaryotes*, ed. E. Rosenberg, E. F.  
656 DeLong, S. Lory, E. Stackebrandt, F. Thompson (Springer, Berlin), 45-73, doi: 10.1007/978-  
657 3-642-39044-9\_266, 2014.
- 658 Lam., P., Lavik, G., Jensen, M. M., van de Vossenberg, J., Schmid, M., Woebken, et al.: Revising  
659 the nitrogen cycle in the Peruvian oxygen minimum zone, *Proc. Natl. Acad. Sci. USA.*, 106,  
660 4752–4757, doi: 10.1073/pnas.0812444106, 2009.
- 661 Larkin, M. A., Blackshields, G., Brown, N. P., Chenna, R., McGettigan, P. A., McWilliam, H., et  
662 al.: Clustal W and Clustal X version 2.0., *Bioinformatics*, 23, 2947–2948, doi:  
663 10.1093/bioinformatics/btm404, 2007. Lee, J., Kim, S. and An, S.: Dynamics of the Physical  
664 and biogeochemical processes during hypoxia in Jinhae Bay, South Korea, *J. Coast. Res.*,  
665 33(4), 854-863, doi: 10.2112/JCOASTRES-D-16-00122.1, 2017.
- 666 Mattes, T. E., Nunn, B. L., Marshall, K. T., Proskurowski, G., Kelley, D. S., Kawka, O. E., et al.:  
667 Sulfur oxidizers dominate carbon fixation at a biogeochemical hot spot in the dark ocean,  
668 *ISME J.*, 7, 2349–2360, doi: 10.1038/ismej.2013.113., 2013.
- 669 McCarthy, M. J., Carini, S. A., Liu, Z., Ostrom, N. E., and Gardner, W. S.: Oxygen consumption  
670 in the water column and sediments of the northern Gulf of Mexico hypoxic zone, *Estuar.  
671 Coast. Shelf Sci.*, 123, 46-53, doi: 10.1016/j.ecss.2013.02.019, 2013.
- 672 Meyer, B., and Kuever, J.: Molecular analysis of the distribution and phylogeny of dissimilatory  
673 adenosine-5'-phosphosulfate reductase-encoding genes (*aprBA*) among sulfur-oxidizing  
674 prokaryotes, *Microbiol.*, 153, 3478–3498, doi: 10.1099/mic.0.2007/008250-0, 2007a.
- 675 Meyer, B., and Kuever, J.: Molecular analysis of the diversity of sulfate-reducing and sulfur-  
676 oxidizing prokaryotes in the environment, using *aprA* as functional marker gene, *Appl.  
677 Environ. Microbiol.*, 73, 7664–7679, doi: 10.1128/AEM.01272-07, 2007b.



- 678 Ministry of Oceans and Fisheries Staff (MOF):. Development of hypoxic water mass restoration  
679 technology in an inner bay, Seoul, Ministry of Oceans and Fisheries, 2015.
- 680 Munson, A., Nedwell, D. B., and Embley, T. M.: Phylogenetic diversity of Archaea in sediment  
681 samples from a coastal salt marsh, *Appl. Environ. Microbiol.*, 63, 4729–4733, 1997.
- 682 Murrell, M.C., and Lehrter, J.: Sediment and lower water column oxygen consumption in the  
683 seasonally hypoxic region of the Louisiana continental shelf, *Estuaries Coasts.*, 34, 912–924,  
684 doi: 10.1007/s12237-010-9351-9, 2011.
- 685 Nadkarni, M. A., Martin, F. E., Jacques, N. A., and Hunter, N.: Determination of bacterial load  
686 by real-time PCR using a broad-range (universal) probe and primers set, *Microbiol.*, 148,  
687 257–266, doi: 10.1099/00221287-148-1-257, 2002.
- 688 Naqvi, S. W., Bange, H. W., Farias, L., Monteiro, P. M., Scranton, M. I., and Zhang, J.: Marine  
689 hypoxia/anoxia as a source of CH<sub>4</sub> and N<sub>2</sub>O, *Biogeosciences*, 7, 2159–2190, doi: 10.5194/bg-  
690 7-2159-2010, 2010.
- 691 Nogales, B., Lanfranconi, M. P., Pina-Villalonga, J. M., and Bosch, R.: Antropogenic  
692 perturbations in marine microbial communities, *FEMS. Microbiol. Rev.*, 35, 275–298, doi:  
693 10.1111/j.1574-6976.2010.00248.x, 2011.
- 694 Purcell, A. M., Mikucki, J. A., Achberger, A. M., Alekhina, I. A., Barbante, C., Christner, B. C.,  
695 et al.: Microbial sulfur transformations in sediments from Subglacial Lake Whillans, *Front.*  
696 *Microbiol.*, 5, 594, doi: 10.3389/fmicb.2014.00594, 2014.
- 697 Ravenschlag, K., Sahm, K., Knoblauch, C., Jorgensen, B. B., and Amann, R.: Community  
698 structure, cellular rRNA content, and activity of sulfate-reducing bacteria in marine arctic  
699 sediments, *Appl. Environ. Microbiol.*, 66, 3592–3602, doi: 10.1128/AEM.66.8.3592-  
700 3602.2000, 2000.



- 701 Rowe, G. T.: Seasonal Hypoxia in the Bottom Water off the Mississippi River Delta, *J. Environ.*  
702 *Qual.*, 30, 281–290, doi: 10.2134/jeq2001.302281x, 2001.
- 703 Shao, M. F., Zhang, T., and Fang, H. H.: Sulfur-driven autotrophic denitrification: diversity,  
704 biochemistry, and engineering applications, *Appl. Microbiol. Biotechnol.*, 88(5), 1027–  
705 1042, doi: 10.1007/s00253-010-2847-1, 2010.
- 706 Stahl, D. A., Fishbain, S., Klein, M., Baker, B. J., and Wagner, M.: Origins and diversification of  
707 sulfate-respiring microorganisms, *Antonie Van Leeuwenhoek.*, 81, 189–195, doi:  
708 10.1023/A:1020506415921, 2002.
- 709 Stewart, F. J., Dalsgaard, T., Young, C. R., Thamdrup, B., Revsbech, N. P., Ulloa, O., et al.:  
710 Experimental incubations elicit profound changes in community transcription in OMZ  
711 bacterioplankton, *PLoS One*, 7, e37118, doi: 10.1371/journal.pone.0037118, 2012.
- 712 Strickland, J. D. H., and Parsons, T. R.: *A practical handbook of seawater analysis*, Ottawa: Alger  
713 Press, 1972.
- 714 Swan, B. K., Ehrhardt, C. J., Reifel, K. M., Moreno, L. I., and Valentine, D. L.: Archaeal and  
715 bacterial communities respond differently to environmental gradients in anoxic sediments of  
716 a California hypersaline lake, the salton sea, *Appl. Environ. Microbiol.*, 76, 757-768, doi:  
717 10.1128/AEM.02409-09, 2010.
- 718 Takai, K., and Horikoshi, K.: Rapid detection and quantification of members of the archaeal  
719 community by quantitative PCR using fluorogenic probes, *Appl. Environ. Microbiol.*, 66,  
720 5066–5072, doi: 10.1128/AEM.66.11.5066-5072.2000, 2000.
- 721 Tamura, K., Peterson, D., Peterson, N., Stecher, G., Nei, M., and Kumar, S.: MEGA6: molecular  
722 evolutionary genetics analysis version 6.0, *Mol. Biol. Evol.*, 30, 2725–2729, doi:  
723 10.1093/molbev/mst197, 2013.





- 724 Tuominen, L.: Comparison of leucine uptake methods and a thymidine incorporation method for  
725 measuring bacterial activity in sediment, *J. Microbiol. Methods.*, 24, 125–134, doi:  
726 10.1016/0167-7012(95)00062-3, 1995.
- 727 Ulloa, O., Canfield, D. E., DeLong, E. F., Letelier, R. M., and Stewart, F. J.: Perspective:  
728 microbial oceanography of anoxic oxygen minimum zones, *Proc. Natl. Acad. Sci. USA.*, 109,  
729 15996–16003, doi: 10.1073/pnas.1205009109, 2012.
- 730 Wagner, M., Roger, A. M., Flax, J. L., Brusseau, G. A., and Stahl, D. A.: Phylogeny of  
731 dissimilatory sulfite reductases supports an early origin of sulfate respiration, *J. Bacteriol.*,  
732 180, 2975–2982, 1998.
- 733 Ward, B. B.: “Nitrification in the Ocean,” in *Nitrification*, ed. B. B. Ward, M. G. Klotz and D. A.  
734 Arp (Washington, DC: ASM press), 325–345, doi: 10.1128/9781555817145.ch13, 2011.
- 735 Watanabe, T., Kojima, H., Takano, Y., and Fukui, M.: Diversity of sulfur-cycle prokaryotes in  
736 freshwater lake sediments investigated using *aprA* as functional marker gene, *Syst. Appl.*  
737 *Microbiol.*, 36, 436–443, doi: 10.1016/j.syapm.2013.04.009, 2013.
- 738 Wright, J. J., Konwar, K. M., and Hallam, S. J.: Microbial ecology of expanding oxygen  
739 minimum zones, *Nat. Rev. Microbiol.*, 10, 381–394, doi: 10.1038/nrmicro2778, 2012.
- 740 Ye, Q., Wu, Y., Zhu, Z., Wang, X., Li, Z., and Zhang, J.: Bacterial diversity in the surface  
741 sediments of the hypoxic zone near the Changjiang Estuary and in the East China Sea,  
742 *Microbiologyopen*, 5, 323–339, doi: 10.1002/mbo3.330, 2016.
- 743 Yu, Y., Lee, C., Kim, J., and Hwang, S.: Group specific primer and probe sets to detect  
744 methanogenic communities using quantitative real-time polymerase chain reaction,  
745 *Biotechnol. Bioeng.*, 89, 670–679, doi: 10.1002/bit.20347, 2005.



**Table 1: List of Jinhae Bay adenosine 5'-phosphosulfate reductase alpha subunit operational taxonomic units (OTUs) and their relatedness to known sulfur-cycle-related groups (T: top, M: middle, B: bottom layers of water and S: sediment).**

OTU type (#)	Sample originated (#)	AA identity (%)	Highest match (accession number)	AA identity (%)	Highest cultured match (accession number)
Sulfur-oxidizing (SOP)- SOP lineage I					
4(14)	T(2), M(2), S(10)	88-99	Uncultured bacterium clone lcm_60 (AKQ24881)	78-94	Gamma proteobacterium SCGC AAA240-C17 (ADX05650)
9(1)	S(1)	84-90	Uncultured prokaryote clone MC-3C 3.5-8cm-10 (AIW55966)	75-88	<i>Olavius algarvensis</i> gamma 3 endosymbiont (CAJ81241)
13(50)	T(24), M(11), B(10), S(5)	82-94	Uncultured prokaryote clone aprE9 (CBH30854)	80-92	Gamma proteobacterium SCGC AAA001-B15(WP_010507240)
21(35)	T(2), M(3), B(3), S(27)	85-95	Uncultured gamma proteobacterium clone bes3.30 (CAT03609)	82-97	<i>Candidatus thibios zoothammicoli</i> strain calvi (ACC95127)
28(1)	B(1)	87-96	Uncultured gamma proteobacterium clone L.S.Fer.APS.12 (CCC58236)	79-95	Bacterium symbiont of <i>Christineconcha regab</i> 225-V5 (AGR49140)
Sulfur-oxidizing prokaryote (SOP) <i>aprA</i> lineage II					
3(16)	T(1), M(1), S(14)	86-98	Uncultured gamma proteobacterium clone bes 3.1 (FM879016)	73-92	Bacteria endosymbiont of <i>Lucinoma</i> aff. <i>kazani</i> clone L8 (AM236338)
29(1)	S(1)	83-98	Uncultured bacterium clone A49 (AFK76430)	67-92	<i>Olavius algarvensis</i> gamma 1 endosymbiont Isolate 5 (CAJ81240)
Gram-positive sulfate-reducing bacteria (SRB) and related <i>Deltaproteobacteria</i>					
1(1)	T(1)	78-89	Uncultured bacterium clone DdH6 (AFV48086)	66-88	<i>Desulfotomaculum kuznetsovii</i> DSM 6115 (AF418152)
7(2)	S(2)	75-92	Uncultured bacterium clone aspA70m14 (ADD84947)	60-92	<i>Gemmatimonas</i> sp. SG8_17 (KPJ93694)
8(1)	S(1)	73-90	Uncultured bacterium clone 28_13 (AGV76884)	63-81	<i>Desulfotomaculum kuznetsovii</i> DSM 6115 (AAL57419)
10(2)	S(2)	71-89	Uncultured bacterium clone lcm_37 (AKQ24858)	62-89	<i>Gemmatimonas</i> sp. SG8_17 (KPJ93694)
12(1)	S(1)	72-93	Uncultured delta proteobacterium clone bes 3.41 (CAT03614)	63-88	<i>Desulfomonile tiedjei</i> DSM 6799 (AAL57429)
14(1)	S(1)	70-91	<i>Gemmatimonas</i> sp. clone SG8_38_2 (KPK65885)	61-91	Delta proteobacterium SM-66-47 (CCC55932)
15(1)	S(1)	76-94	Uncultured bacterium clone lcm_13 (AKQ24834)	66-88	<i>Desulfotomaculum geothermicum</i> DSM 3669 (AAL57382)
17(1)	S(1)	73-95	Uncultured bacterium clone A079 (ADW77112)	63-79	<i>Desulfotomaculum kuznetsovii</i> DSM 6115 (AAL57419)
18(1)	S(1)	71-88	Uncultured bacterium clone lcm_13 (AKQ24834)	62-79	<i>Desulfotomaculum geothermicum</i> DSM 3669 (AAL57382)



**Table 1 (Continued)**

OTU type (#)	Sample originated (#)	AA identity (%)	Highest match (accession number)	AA identity (%)	Highest cultured match (accession number)
19(2)	S(2)	73-88	Uncultured delta proteobacterium clone bcs_3.41 (CAT03614)	62-85	<i>Desulfomonile tiedjei</i> DSM 6799 (AAL57429)
20(1)	S(1)	68-96	Uncultured bacterium clone Ha_3.5m_57 (BAO79242)	58-82	Delta proteobacterium SM-66-64 (CCC55931)
22(1)	S(1)	74-92	Uncultured bacterium clone 28_13 (AGV76884)	64-81	<i>Desulfotomaculum kuznetsovii</i> DSM 6115 (AAL57419)
23(1)	S(1)	73-86	Uncultured <i>Firmicutes</i> bacterium clone T8- <i>aprA</i> -22 (AFC36470)	63-82	<i>Desulfotomaculum kuznetsovii</i> DSM 6115 (AAL57419)
24(2)	S(2)	76-95	Uncultured sulfate-reducing bacterium (CAJ31201)	64-93	<i>Gemmatimonas</i> sp. SG8_17 (KPJ93694)
26(2)	S(2)	74-97	Uncultured bacterium clone C6507_ <i>aprA</i> _7B101 (ACM47772)	74-97	<i>Nitrospira bacterium</i> SG8_3 (KPK16323)
30(1)	S(1)	70-96	Uncultured bacterium clone 89_APS30_EDS_640 (ADJ38098)	59-82	<i>Bacteroides</i> sp. SM23_62_1 (KPK79634)
31(1)	S(1)	72-84	Uncultured bacterium clone GoM_ <i>AprA</i> _3 (CCB84471)	63-78	Delta proteobacterium SM-66-47 (CCC55932)
32(1)	S(1)	73-98	Uncultured bacterium clone SKCK0606_1H2_6 (BAQ03184)	65-84	<i>Desulforhabdus amnigena</i> DSM 10338 (AAL57406)
33(1)	S(1)	75-89	Uncultured bacterium clone 1cm_50 (AKQ24871)	64-86	Delta proteobacterium SM-66-47 (CCC55932)
Thermophilic sulfate reducing bacteria (SRB)					
25(1)	S(1)	63-81	Uncultured prokaryote clone CVA- <i>aprA</i> -28 (CCG27943)	58-76	<i>Thermodesulfobivrio islandicus</i> DSM 12570 (AAL57380)
Deltaproteobacterial sulfate reducing bacteria (SRB)					
2(5)	T(1), M(2), S(2)	73-94	Uncultured bacterium clone PB70 (KF788937)	69-76	<i>Desulfonatronovibrio hydrogenovorans</i> DSM 9292 (AF418111)
5(5)	T(1), S(4)	89-99	Uncultured delta proteobacterium (EU265806)	78-95	<i>Desulfobulbus elongates</i> clone DSM 2908 (AF418146)
6(1)	S(1)	81-96	Uncultured bacterium clone BSC/K0903_1H3_21 (BAQ03029)	76-95	<i>Nitrospira bacterium</i> SG8_3 (LJNR01000453)
11(8)	S(8)	86-97	Uncultured bacterium clone 1cm_42 (AKQ24863)	76-95	<i>Olavius algarvensis</i> delta 1 endosymbiont isolate 5 (CAJ81242)
16(5)	S(5)	83-99	Uncultured bacterium clone 1cm_1 (AKQ24822)	73-97	<i>Desulfofustis glycolicus</i> DSM 9705 (AAL57397)
27(1)	B(1)	77-95	Uncultured bacterium clone 1cm_17 (AKQ24838)	67-95	<i>Desulfobacter curvatus</i> DSM 3379 (AAL57374)



**Figure 1: Temporal variations in surface and bottom oxygen saturation (%) and water temperature (°C) from January–December 2015 at each time period (S1, S5: solubility period, H2, H3, H4: hypoxia period). The arrows show the five sampling dates for the microbial study (S1, H2A, H2B, H3A, and H3B) in Jinhae Bay.**

**Figure 2: Vertical profiles of (A) temperature, (B) dissolved oxygen, (C)  $\text{NO}_3^-$ , and (D)  $\text{NH}_4^+$  during normoxic (Jan, Apr, May, Nov) and hypoxic (Jun, Jul, Sep) periods at Jinhae Bay.**

**Figure 3: Copy numbers of prokaryotes (bacteria and archaea) during quantitative polymerase chain reaction analysis and water-column oxygen demand in the (A) top, middle, and bottom layers, and (B) sediment oxygen demand of Jinhae Bay.** Each sample was collected across seasonal time periods from January to June. S1, S5: solubility period, H2, H3, H4: hypoxia period, See Fig. 1 for sample dates.

**Figure 4: Copy numbers of bacterial, archaeal, and *adenosine 5'-phosphosulfate reductase alpha subunit (aprA)* genes in the (A) top, (B) middle, and (C) bottom layers of the water column or in the (D) sediment of Jinhae Bay.** (BAC = bacterial 16S ribosomal RNA (rRNA), ARC = archaeal 16S rRNA and APR = *aprA* gene). See Fig. 1 for sample dates.

**Figure 5: Phylogenetic analysis of *adenosine 5'-phosphosulfate reductase alpha subunit (aprA)* gene sequences obtained from Jinhae Bay.** The *aprA* gene sequence from *Pyrobaculum aerophilum* (GenBank accession number: AAL64282) was used as an outgroup. Bootstrap values (1000 samples) are shown on the corresponding nodes.



**Figure 6: Operational taxonomic units (OTUs) occurred at each period of hypoxia in the water column for (A) top, (B) middle, (C) bottom layers, and (D) surface sediment. Each OTU was classified as either a sulfide-oxidizing prokaryote or a sulfate-reducing prokaryote.**

See text for details.



**Figure 1: Temporal variations in surface and bottom oxygen saturation (%) and water temperature (°C) from January–December 2015 at each time period (S1, S5: solubility period, H2, H3, H4: hypoxia period). The arrows show the five sampling dates for the microbial study (S1, H2A, H2B, H3A, and H3B) in Jinhae Bay.**

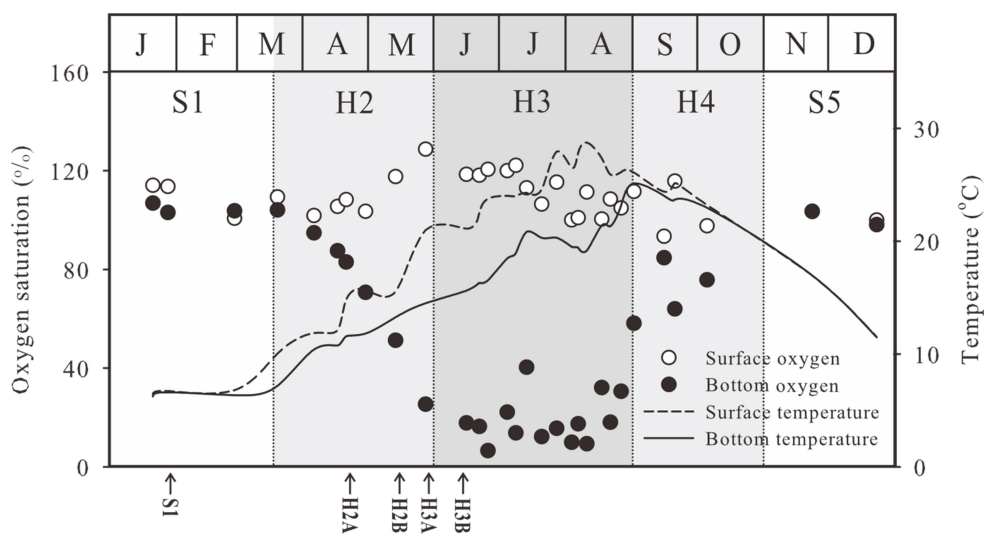




**Figure 2: Vertical profiles of (A) temperature, (B) dissolved oxygen, (C)  $\text{NO}_3^-$ , and (D)  $\text{NH}_4^+$  during normoxic (Jan, Apr, May, Nov) and hypoxic (Jun, Jul, Sep) periods at Jinhae Bay.**

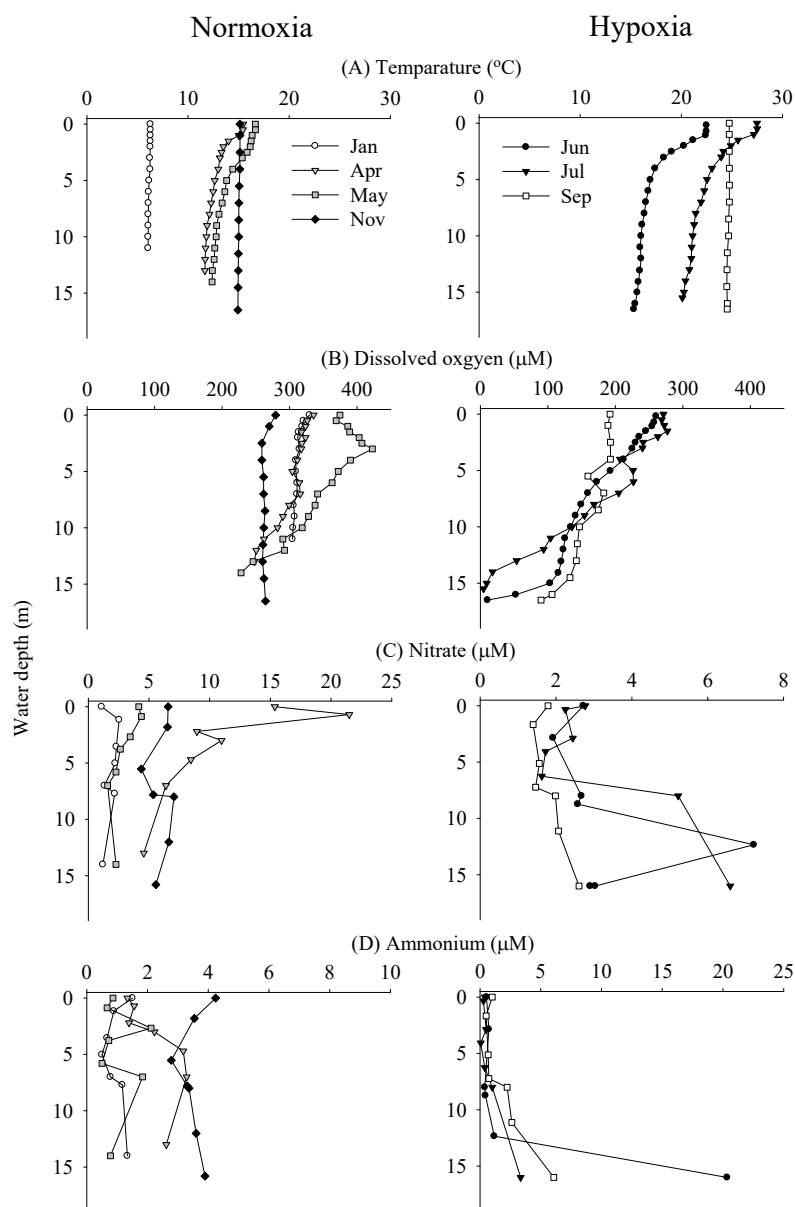




**Figure 3: Copy numbers of prokaryotes (bacteria and archaea) during quantitative polymerase chain reaction analysis and water-column oxygen demand in the (A) top, middle, and bottom layers, and (B) sediment oxygen demand of Jinhae Bay. Each sample was collected across seasonal time periods from January to June. S1, S5: solubility period, H2, H3, H4: hypoxia period, See Fig. 1 for sample dates.**

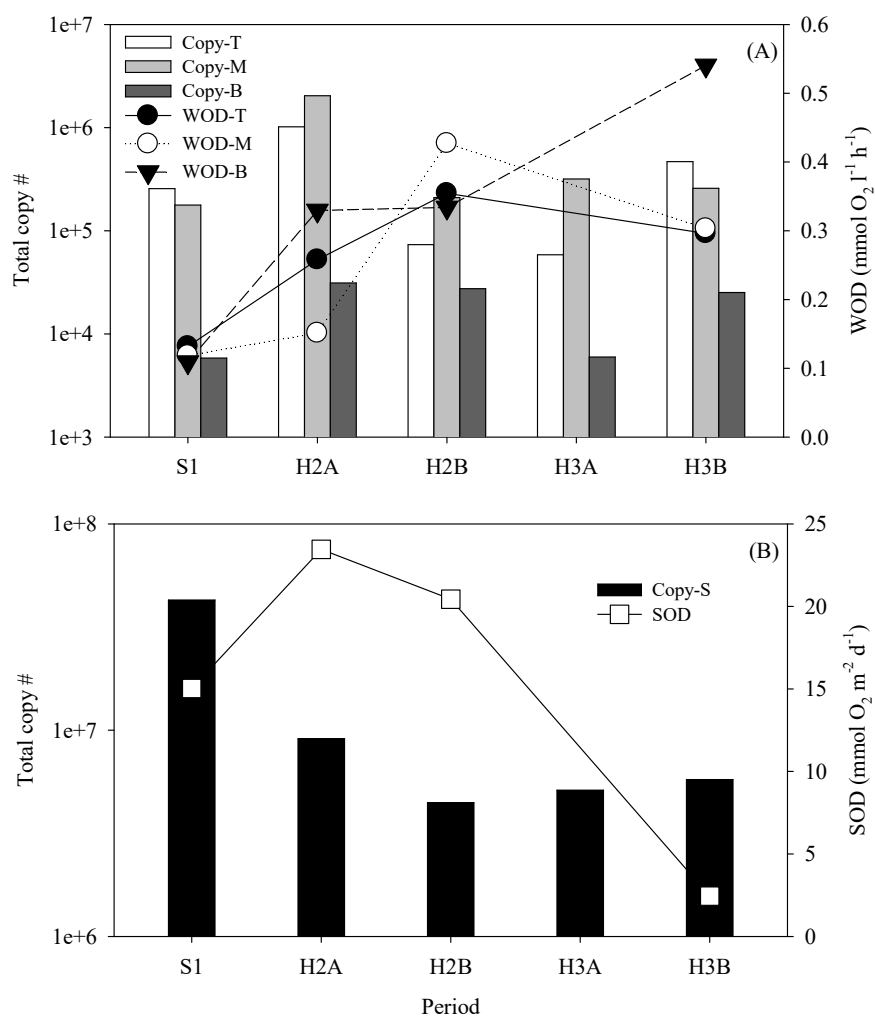






**Figure 4: Copy numbers of bacterial, archaeal, and *adenosine 5'-phosphosulfate reductase alpha subunit (aprA)* genes in the (A) top, (B) middle, and (C) bottom layers of the water column or in the (D) sediment of Jinhae Bay. (BAC = bacterial 16S ribosomal RNA (rRNA), ARC = archaeal 16S rRNA and APR = *aprA* gene). See Fig. 1 for sample dates.**

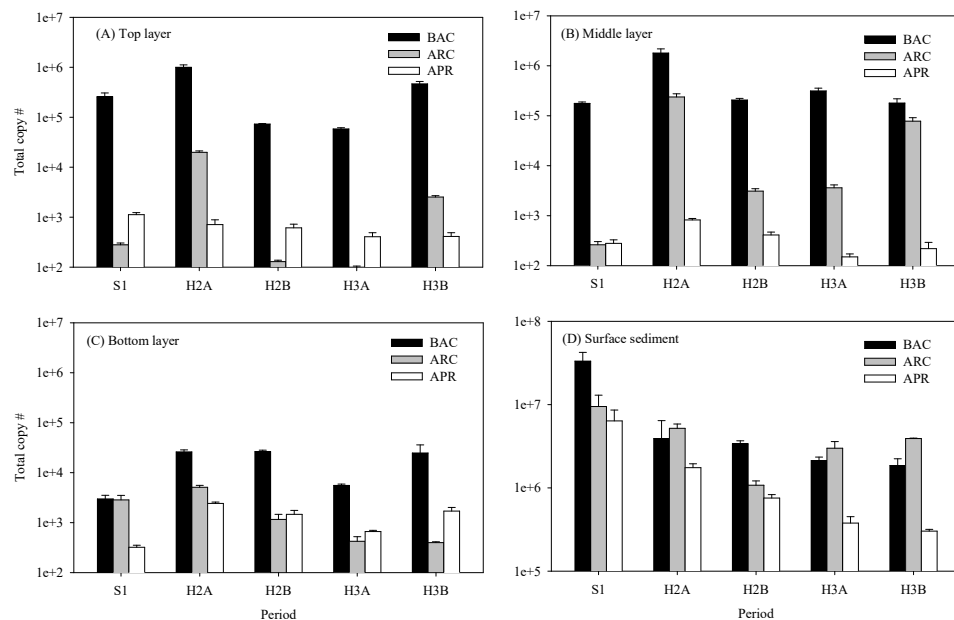




**Figure 5: Phylogenetic analysis of adenosine 5'-phosphosulfate reductase alpha subunit (*aprA*) gene sequences obtained from Jinhae Bay.** The *aprA* gene sequence from *Pyrobaculum aerophilum* (GenBank accession number: AAL64282) was used as an outgroup. Bootstrap values (1000 samples) are shown on the corresponding nodes.

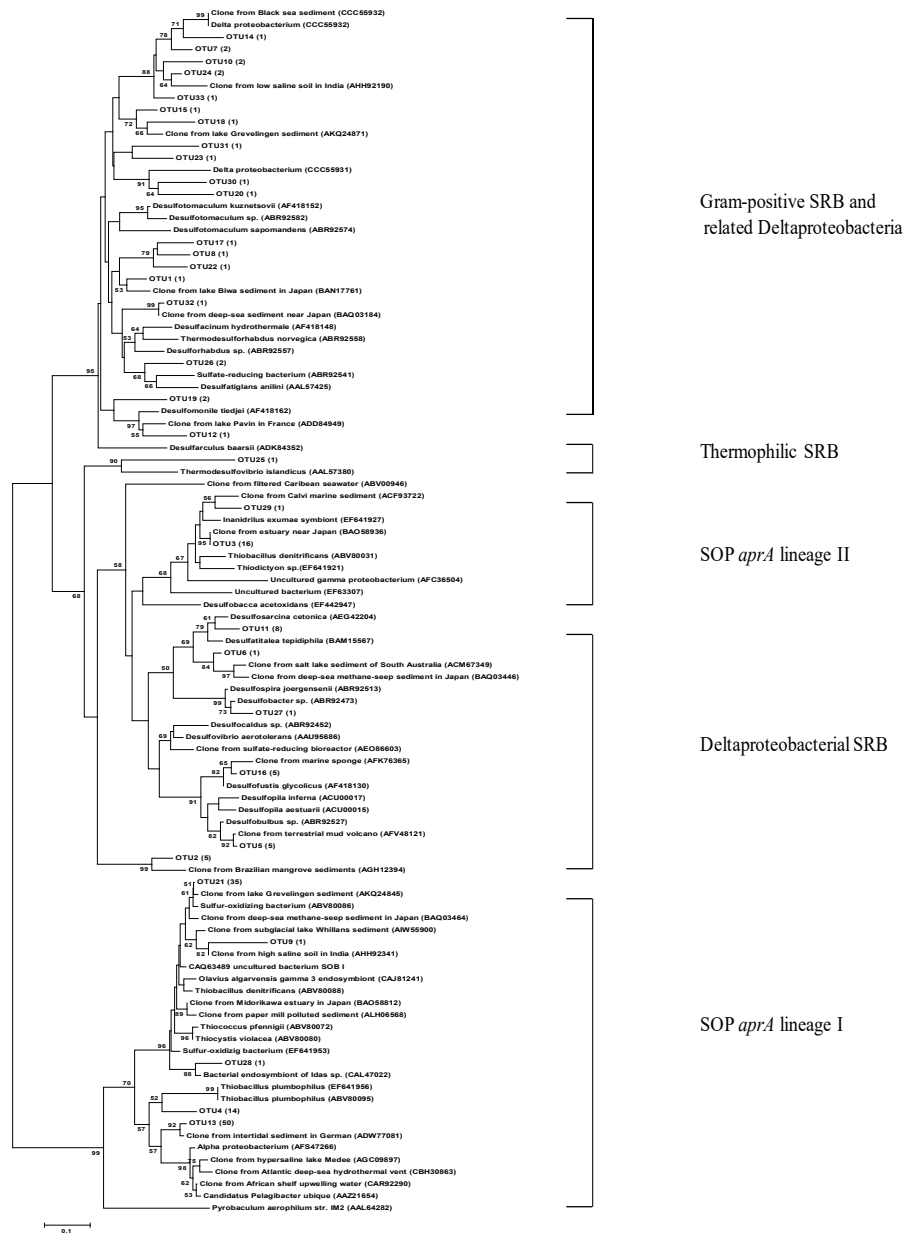




**Figure 6: Operational taxonomic units (OTUs) occurred at each period of hypoxia in the water column for (A) top, (B) middle, (C) bottom layers, and (D) surface sediment. Each OTU was classified as either a sulfide-oxidizing prokaryote or a sulfate-reducing prokaryote.**

See text for details.

